Inorg. Chem. **2008**, *47*, 1037–1043

Synthesis, Structures, and Magnetic Properties of Metal-Coordination Polymers with Benzenepentacarboxylate Linkers

Xin-Yi Wang and Slavi C. Sevov*

Department of Chemistry and Biochemistry, University of Notre Dame, Notre Dame, Indiana 46556

Received September 24, 2007

Three hybrid organic–inorganic coordination polymers with benzenepentacarboxylate (BPCA) linkers, $[Co_3(C_6H(COO)_5)(OH)(H_2O)_3]$ (**1-Co**), $[Zn_3(C_6H(COO)_5)(OH)(H_2O)_3]$ (**2-Zn**), and $[Co_5(C_6H(COO)_5)_2(H_2O)_{12}]\cdot(H_2O)_{12}$ (**3-Co**), were synthesized hydrothermally and were characterized structurally and magnetically. **1-Co** and **2-Zn** are isostructural [*C*2/*c*; $Z = 8$; **1-Co**, $a = 19.5350(6)$ Å, $b = 10.4494(4)$ Å, and $c = 13.2353(5)$ Å, $\beta = 97.2768(8)°$; **2-Zn**, $a = 19.5418(9)$ Å, $b = 10.3220(10)$ Å, and $c = 13.4660(10)$ Å, $\beta = 98.455(10)°$] with three-dimensional structures that contain $[M_6]$ secondary building units bridged by BPCA ligands. A different cobalt-based compound, **3-Co**, forms at lower pH and lower reaction temperature. Its structure [$P2_1/c$; $Z = 2$; $a = 12.6162(2)$ Å, $b = 11.3768(2)$ Å, and $c = 15.3401(3)$ Å, $\beta = 91.539(1)°$] is a more loosely packed framework with free (noncoordinated) carboxylic groups pointing at water-filled cavities in the framework. The magnetic phase diagram of **1-Co** established through detailed magnetic measurements shows a metamagnetic transition below $T_N = 3.8$ K. The less-packed compound **3-Co**, on the other hand, remains paramagnetic above 1.9 K. The three compounds are the first examples of coordination polymers with benzenepentacarboxylate linkers and fill the gap of coordination polymers involving benzenepolycarboxylate linkers of the general type $C_6H_{6-n}(COOH)_n$, where $n = 2–6$.

Introduction

Hybrid organic−inorganic coordination polymers constructed of transition-metal ions bridged by organic linkers are of great interest for many reasons, not the least of which is their suitability for rational supramolecular engineering.[1] In addition to their numerous potential applications such as ion exchange,[2] hydrogen storage,[3] nonlinear optics,[4] conductivity,[5] the coordination polymers have recently attracted attention due to their potential for interesting magnetic properties.[6] Despite the low critical temperatures of many of them and the slim chance for real applications as magnetic materials, studying the magnetic properties of coordination polymers is advantageous for a few reasons. For example, their numerous structure types and topologies provide for easy magneto−structural correlations, while their multicomponent structures improve the chances for finding multifunctional materials with magnetic properties.[7]

Within the coordination polymers, those with polycarboxylate linkers form a special and very important group, because of their abundance, diversity, multifunctionality, and overall stability.[8] The linkers vary from the very small formate,[9] oxalate,[10] and malonate,[11] to the very bulky examples of 2,7-pyrenedicarboxylate and [1,1′:4′,1″-terphenyl]-4,4″-dicarboxylate.[12] Among them, the ring-based polycarboxylic acids with cores of, for example, benzene, THF, and cyclopentane with formulas $C_6H_{6-n}(COOH)_n$ ($n = 2−6$),

* To whom correspondence should be addressed. E-mail: ssevov@nd.edu.

(1) (a) Reed, C. A., Ed. Special issue on Molecular Architectures. *Acc. Chem. Res.* **2005**, *38*, 215−378. (b) Cheetham, A. K.; Rao, C. N. R.; Feller, R. K. *Chem. Commun.* 2006, 4780−4795. (c) Moulton, B.; Zaworotko, M. J. *Chem. Rev.* **2001**, *101*, 1629−1658.
(2) Kitagawa, S.; Kitaura, R.; Noro, S. *Angew. Chem., Int. Ed.* **2004**, *43*, 2334−2375.
(3) Rowsell, J. C. C.; Yaghi, O. M. *Angew. Chem., Int. Ed.* **2005**, *44*, 4670−4679.
(4) Innocenzi, P.; Lebeau, B. *J. Mater. Chem.* **2005**, *15*, 3821−3831.
(5) Coronado, E.; Day, P. *Chem. Rev.* **2004**, *104*, 5419.;
(6) (a) Miller, J. S., Drillon, M., Eds. *Magnetism: Molecules to Materials*; Wiley-VCH: New York, 2002−2005; Vol. I−V. (b) Thompson, L. K., Ed. Special issue on Magnetism−Molecular and Supramolecular Perspectives. *Coord. Chem. Rev.* **2005**, *249*, 2549−2730. (c) Rabu, P.; Drillon, M. *Adv. Eng. Mater.* **2003**, *5*, 189−210.
(7) (a) Sato, O.; Tao, J.; Zhang, Y. Z. *Angew. Chem., Int. Ed.* **2007**, *46*, 2152−2187. (b) Decurtins, S.; Pellaux, R.; Antorrena, G.; Palacio, F. *Coord. Chem. Rev.* **1999**, *190−192*, 841. (c) Gütlich, P.; Garcia, Y.; Woike, T. *Coord. Chem. Rev.* **2001**, *219−221*, 839.
(8) (a) Maspoch, D.; Ruiz-Molina, D.; Veciana, J. *Chem. Soc. Rev.* **2007**, *36*, 770−818. (b) Rao, C. N. R.; Natarajan, S.; Vaidhyanathan, R. *Angew. Chem., Int. Ed.* **2004**, *43*, 1466.(c) Guillou, N.; Livage, C.; Férey, G. *Eur. J. Inorg. Chem.* **2006**, 4963−4978.

10.1021/ic701893z CCC: $40.75
Published on Web 12/21/2007

$C_4H_{8-n}O(COOH)_n$ ($n = 2-4$), and $C_5H_{10-n}(COOH)_n$ ($n = 2-5$), respectively, should be excellent linkers for building such networks, because of their capability to serve as multiconnecting ligands and to "engineer" novel structures. However, besides the enormous attention focused on structures and properties with benzene di-, tri-, and tetracarboxylate linkers $C_6H_4(COO^-)_2$, $C_6H_3(COO^-)_3$, and $C_6H_2(COO^-)_4$, respectively,[12,13] and their multiring derivatives, there are very few reports on compounds involving the corresponding penta- and hexacarboxylates or linkers with THF and cyclopentane cores. As a matter of fact, according to the 2007 version of the Cambridge Structural Database, not a single example with a pentacarboxylate linker is known, i.e., a metal−organic polymer synthesized with benzenepentacarboxylic acid (H_5BPCA), $C_6H(COOH)_5$. One likely reason for being overlooked is the tendency for polycarboxylates with four and more carboxylic groups to form more densely packed structures because of their multitude of coordinating sites. However, such multicarboxylate linkers, especially those with relatively small organic cores, such as benzene and THF, could be advantageous, because of their potential to retain free noncoordinated functional groups, carboxylates in this case, in the resulting framework. The reason for this is the spatial overcrowding and high concentration of functional groups in a very small volume that leads to steric inability to stuff enough metal centers around the small molecule in order to satisfy all functional groups. Such frameworks may have special properties due to the noncoordinated groups, especially if they are accessible via channels in the framework structure.[14] Another structural feature that polycarboxylates with four or more groups could potentially provide is clustering and close proximity of the metal centers that, in turn, may lead to better magnetic coupling. For example, we have already shown that frameworks made of Mn, Co, Cu, or Zn linked by tetrahydrofurantetracarboxylate linkers exhibit interesting structures and magnetic properties.[15]

With the above considerations in mind, we explored for metal-coordination polymers of Mn, Co, Ni, Cu, and Zn interconnected by BPCA linkers. Here we report the hydrothermal synthesis and structural and magnetic characterization of three such compounds: $[Co_3(C_6H(COO)_5)(OH)(H_2O)_3]$ (**1-Co**), $[Zn_3(C_6H(COO)_5)(OH)(H_2O)_3]$ (**2-Zn**), and $[Co_5(C_6H(COO)_5)_2(H_2O)_{12}]\cdot(H_2O)_{12}$ (**3-Co**).

Experimental Section

H_5BPCA (98%) was purchased from TCI America and used as received.

Synthesis of $[Co_3(C_6H(COO)_5)(OH)(H_2O)_3]$. 1-Co was synthesized hydrothermally in a 23 mL Teflon-lined autoclave heated at 195 °C for 3 days. The reaction mixture contained $CoCl_2\cdot 6H_2O$ (60 mg, 0.25 mmol), H_5BPCA (30 mg, 0.10 mmol), NaOH (0.5 mL of 1 M solution, 0.5 mmol), and 6 mL of H_2O (final pH ~5.0). The crystals of the single-phase product were column-shaped and purple. They were filtered from the mother liquid, washed with water, and allowed to air-dry (about 40 mg, yield of ca. 70% based on H_5BPCA).

Synthesis of $[Zn_3(C_6H(COO)_5)(OH)(H_2O)_3]$. 2-Zn was obtained from a similar reaction carried out at 125 °C for 2 days. The autoclave was loaded with $ZnCl_2$ (95 mg, 0.70 mmol), H_5-BPCA (45 mg, 0.15 mmol), NaOH (0.8 mL of 1 M solution, 0.8 mmol), and 3 mL of H_2O (final pH ~4.0). The reaction produced several colorless crystals that were collected and allowed to air-dry (about 18 mg, yield of ca. 30% based on H_5BPCA).

Synthesis of $[Co_5(C_6H(COO)_5)_2(H_2O)_{12}]\cdot(H_2O)_{12}$. This compound, **3-Co**, was obtained from a reaction similar to the one carried out for **1-Co** but at lower temperature, 135 °C for 3 days, and lower pH of 4. The reaction mixture was made of $CoCl_2\cdot 6H_2O$ (180 mg, 0.75 mmol), H_5BPCA (45 mg, 0.15 mmol), NaOH (0.7 mL of 1 M solution, 0.7 mmol), and 3 mL of H_2O. The compound crystallizes as pale-red plates that coexist with amorphous fine powder. The crystals were manually separated from the powder under microscope and washed with water (about 15 mg, yield of ca. 15% based on H_5BPCA).

Structure Determination. The data set for **2-Zn** was collected on an Enraf-Nonius CAD4 diffractometer at room temperature ($\theta_{max} = 25°$) while those for **1-Co** and **3-Co** were collected on a Bruker APEX-II diffractometer with a CCD area detector at 100 K ($\theta_{max} = 27.5°$), all with Mo Kα radiation ($\lambda = 0.710\ 73$ Å). The structures were solved by direct methods and refined by a full-matrix least-squares technique based on F^2 using the SHELXL97 program.[16] Details of the data collections and structure refinements are presented in Table 1 while all metal−ligand distances are listed in Table 2.

(9) (a) Wang, X. Y.; Wang, Z. M.; Gao, S. *Chem. Commun.* **2007**, published on Web 8/20/2007, DOI: 10.1039/b708122g. (b) Wang, Z. M.; Zhang, B.; Zhang, Y. J.; Kurmoo, M.; Liu, T.; Gao, S.; Kobayashi, H. *Polyhedron* **2007**, *26*, 2207−2215. (c) Wang, Z. M.; Zhang, Y. J.; Liu, T.; Kurmoo, M.; Gao, S. *Adv. Funct. Mater.* **2007**, *17*, 1523−1536. (d) Wang, X. Y.; Gan, L.; Zhang, S. W.; Gao, S. *Inorg. Chem.* **2004**, *43*, 4615. (e) Wang, X. Y.; Wang, Z. M.; Gao, S. *Chem. Commun.* **2007**, 1127. (f) Wang, X. Y.; Wei, H. Y.; Wang, Z. M.; Gao, S.; Chen, Z. D. *Inorg. Chem.* **2005**, *44*, 572.

(10) (a) Gruselle, M.; Train, C.; Boubekeur, K.; Gredin, P.; Ovanesyan, N. *Coord. Chem. Rev.* **2006**, *250*, 2491−2500. (b) Pilkington, M.; Decurtins, S. In *Magnetism: Molecules to Materials II*; Miller, J. S., Drillon, M., Eds.; Wiley-VCH: New York, 2002; p 339.

(11) Rodríguez-Martín, Y.; Hernández-Molina, M.; Delgado, F. S.; Pasán, J.; Ruiz-Pérez, C.; Sanchiz, J.; Lloret, F.; Julve, M. *CrystEngComm* **2002**, *4*, 522−535.

(12) For examples: (a) Eddaoudi, M.; Kim, J.; Rosi, N.; Vodak, D.; Wachter, J.; O'Keeffe, M.; Yaghi, O. M. *Science* **2002**, *295*, 469−472. (b) Han, S. S.; Goddard, W. A., III. *J. Am. Chem. Soc.* **2007**, *129*, 8422−8423. (c) Rosi, N. L.; Kim, J.; Eddaoudi, M.; Chen, B. L.; O'Keeffe, M.; Yaghi, O. M. *J. Am. Chem. Soc.* **2005**, *127*, 1504−1518.

(13) For $n = 2$: (a) Go, Y. B.; Wang, X. Q.; Anokhina, E. V.; Jacobson, A. J. *Inorg. Chem.* **2004**, *43*, 5360−5367. (b) Chen, P. K.; Che, Y. X.; Zheng, J. M.; Batten, S. R. *Chem. Mater.* **2007**, *19*, 2162−2167. (c) Moulton, B.; Lu, J. J.; Hajndl, R.; Hariharan, S.; Zaworotko, M. J. *Angew. Chem., Int. Ed.* **2002**, *41*, 2821−2824. (d) Gu, X. J.; Xue, D. F. *Cryst. Growth. Des.* **2006**, *6*, 2551−2557. For $n = 3$: (e) Xie, L. H.; Liu, S. X.; Gao, B.; Zhang, C. D.; Sun, C. Y.; Li, D. H.; Su, Z. M. *Chem. Commun.* **2005**, 2402−2404. (f) Prior, T. J.; Bradshaw, D.; Teat, S. J.; Rosseinsky, M. J. *Chem. Commun.* **2003**, 500−501. For $n = 4$: (g) Kumagai, H.; Chapman, K. W.; Kepert, C. J.; Kurmoo, M. *Polyhedron* **2003**, *22*, 1921−1927. (h) Kumagai, H.; Kepert, C. J.; Kurmoo, M. *Inorg. Chem.* **2002**, *41*, 3410−3422. (i) Murugavel, R.; Krishnamurthy, D.; Sathiyendiran, M. *Dalton Trans.* **2002**, 34−39. For $n = 6$: (j) Yang, E.; Zhang, J.; Li, Z. J.; Gao, S.; Kang, Y.; Chen, Y. B.; Wen, Y. H.; Yao, Y. G. *Inorg. Chem.* **2004**, *43*, 6525−6527. (k) Kumagai, H.; Oka, Y.; Akita-Tanaka, M.; Inoue, K. *Inorg. Chim. Acta* **2002**, *332*, 176−180. And references there in.

(14) Yaghi, O. M.; Li, H.; Groy, T. L. *J. Am. Chem. Soc.* **1996**, *118*, 9096−9101.

(15) (a) Hanson, K.; Calin, N.; Bugaris, D.; Scancella, M.; Sevov, S. C. *J. Am. Chem. Soc.* **2004**, *126*, 10502−10503. (b) Wang, X. Y.; Sevov, S. C. *Chem. Mater.* **2007**, *19*, 3763−3766. (c) Wang, X. Y.; Scancella, M.; Sevov, S. C. *Chem. Mater.* **2007**, *19*, 4506−4513.

(16) *SHELXTL*, version 5.1; Bruker Analytical Systems: Madison, WI, **1997**.

Table 1. Crystallographic Data for Compounds **1-Co**, **2-Zn**, and **3-Co**

compound	**1-Co**	**2-Zn**	**3-Co**
formula	$C_{11}H_8O_{14}Co_3$	$C_{11}H_8O_{14}Zn_3$	$C_{22}H_{50}O_{44}Co_5$
M_r (g mol^{-1})	540.96	560.28	1313.27
crystal system	monoclinic	monoclinic	monoclinic
space group	*C*2/*c*	*C*2/*c*	$P2_1/c$
a (Å)	19.5350(6)	19.5418(9)	12.6162(2)
b (Å)	10.4494(4)	10.3220(10)	11.3768(2)
c (Å)	13.2353(5)	13.4660(10)	15.3401(3)
β (deg)	97.2768(8)	98.455(10)	91.5390(10)
V (Å^3)	2680.0(2)	2686.7(4)	2201.0(7)
Z	8	8	2
ρ_{calcd} (g cm^{-3})	2.682	2.770	1.982
μ(Mo Kα) (mm^{-1})	3.766	5.409	1.978
R1/wR2 ($I > 2\sigma(I)$)[a]	0.0237/0.0267	0.0406/0.0559	0.0336/0.0437
R1/wR2 (all data)[a]	0.0669/0.0681	0.0983/0.1069	0.0790/0.0828

[a] R1 = $[\sum||F_o| - |F_c||]/\sum|F_o|$; wR2 = $\{[\sum w[(F_o)^2 - (F_c)^2]^2]/[\sum w(F_o^2)^2]\}^{1/2}$; $w = [\sigma^2(F_o)^2 + (AP)^2 + BP]^{-1}$, where $P = [(F_o)^2 + 2(F_c)^2]/3$.

Table 2. The M−O Bond Lengths (Å) for Compounds **1-Co**, **2-Zn**, and **3-Co**

		1-Co			
Co1−O5	2.0432(15)	Co1−O11	2.0491(15)	Co1−O10	2.0813(15)
Co1−O8	2.0952(16)	Co1−O13	2.1411(16)	Co1−O14	2.1492(18)
Co2−O11	2.0175(17)	Co2−O9	2.0625(15)	Co2−O2	2.0859(15)
Co2−O7	2.1195(15)	Co2−O9	2.1777(17)	Co2−O14	2.3477(17)
Co3−O1	2.0175(15)	Co3−O6	2.0258(15)	Co3−O3	2.0866(17)
Co3−O11	2.1056(15)	Co3−O12	2.1488(15)	Co3−O7	2.2061(16)
		2-Zn			
Zn1−O5	2.071(4)	Zn1−O11	2.065(4)	Zn1−O10	2.128(4)
Zn1−O8	2.076(4)	Zn1−O13	2.091(4)	Zn1−O14	2.073(4)
Zn2−O11	2.003(4)	Zn2−O9	1.972(4)	Zn2−O2	1.950(4)
Zn2−O7	2.025(4)	Zn2−O9	2.334(4)		
Zn3−O1	2.050(4)	Zn3−O6	2.052(4)	Zn3−O3	2.030(4)
Zn3−O11	2.052(4)	Zn3−O12	2.073(4)	Zn3−O7	2.2061(16)
		3-Co			
Co1−O1	2.0842(18)	Co1−O1	2.0842(18)	Co1−O11	2.0886(19)
Co1−O11	2.0886(19)	Co1−O12	2.095(2)	Co1−O12	2.094(2)
Co2−O10	2.0169(18)	Co2−O14	2.0554(19)	Co2−O3	2.0844(18)
Co2−O13	2.1134(19)	Co2−O2	2.1369(19)	Co2−O6	2.1517(18)
Co3−O15	1.9952(18)	Co3−O9	2.0247(18)	Co3−O16	2.1121(19)
Co3−O5	2.1131(18)	Co3−O3	2.1219(18)	Co3−O6	2.2036(18)

Magnetic Measurements. Measurements of the temperature dependence of the magnetic susceptibilities and the field dependence of the magnetizations of polycrystalline samples of **1-Co** and **3-Co** were performed on a Quantum Design MPMS SQUID system. All experimental magnetic data were corrected for the diamagnetism of the sample holders and of the constituent atoms (Pascal's tables).

Results and Discussion

Structures of 1-Co and 2-Zn. Although synthesized at different temperatures, concentrations, and pH, these two compounds are isostructural. The structure is very complex (Figure 1) and can be viewed as an extended three-dimensional network made of secondary building units (SBUs) of six metal centers, [M_6], fully deprotonated $BPCA^{5-}$ linkers, OH^- anions, and coordinated water molecules. The metal centers are distributed among three crystallographically unique sites at general positions. Two of them, M1 and M3, are octahedrally coordinated by oxygen atoms (Figure 1a, Table 2): M1 by three atoms from $BPCA^{5-}$, two water molecules (O13, O14), and one OH^- group (O11), and M3 by four atoms from $BPCA^{5-}$, one water molecule (O12), and one OH^- anion (O11). The coordination of the M2 position, on the other hand, is somewhat different in **1-Co** compared to **2-Zn**. That coordination in the former is of a very distorted octahedron made of four oxygen atoms from $BPCA^{5-}$, one OH^- group (O11), and a very weakly coordinated water (O14) with a long Co2−O14 distance of 2.35 Å. Zn2 in **2-Zn**, on the other hand, is clearly in a trigonal bipyramidal environment with a Zn2−O14 distance of 3.31 Å that is beyond any Zn−O interactions.

The fully deprotonated $BPCA^{5-}$ uses nine of its ten oxygen atoms to coordinate to ten metal atoms and bridge them in a variety of bridging modes (Figure 1a). Two of the carboxylic groups, O1−C7−O2 and O5−C9−O6, are in syn−syn mode and bridge within the pairs M2−M3 and M1−M3, while another two, O7−C10−O8 and O9−C11−O10, bridge three M centers in the syn−syn/anti and anti−syn/anti modes, respectively. The last one, O3−C8−O4, does not act as a bridge, because it coordinates to only one metal center, M3. The hydroxyl group in the structure acts as a μ_3-bridge between M1, M2, and M3. As a result of all these connecting modes, the structure exhibits well-defined clusters of six metal centers that are bridged by oxygen atoms within the clusters (Figure 1b). The distances between the metal centers within the SBUs are very short; for example, in **1-Co** they are Co1−Co2 = 3.32 Å, Co2−Co3 = 3.19 Å, Co1−Co3 = 3.72 Å, and Co2−Co2A = 3.28 Å. Such single-oxygen and carboxylate bridges are known to transmit magnetic coupling between adjacent centers very efficiently.[17]

The [M_6] SBUs are bridged by pairs of carboxylate groups (O7−C10−O8) to form one-dimensional tapes along the *c*-direction (Figure 1c). These tapes are then linked by BPCA ligands along the other two directions to form the three-dimensional structure shown in Figure 1d. Since the organic residues of the BPCA linkers are unlikely to transmit magnetic coupling, the magnetic interaction within the SBUs and within the tapes of SBUs are expected to dominate the magnetic properties at high temperatures.

Structure of 3-Co. Unlike the well-packed structures of **1-Co** and **2-Zn**, this compound has a more open framework with plenty of space for lattice water molecules in its cavities (Figure 2). The main difference between the stoichiometries of **1-Co** and **3-Co**, $[Co_3(C_6H(COO)_5)(OH)(H_2O)_3]$ and $[Co_5(C_6H(COO)_5)_2(H_2O)_{12}]\cdot(H_2O)_{12}$, respectively, is the absence of μ_3-OH^- in the latter. This and the less-packed structure confirm that lower reaction temperatures and less basic conditions lead to less packed structures, as previously observed in other multicarboxylate systems.[13h,18] The three-dimensional framework of $[Co_5(C_6H(COO)_5)_2(H_2O)_{12}]\cdot(H_2O)_{12}$ has three crystallographically unique cobalt sites, of which Co1 is at an inversion center while the other two are at general positions (Figure 2a). All of them are

(17) (a) Kahn, O. *Molecular Magnetism*; VCH Publishers: New York, 1993. (b) Carlin, R. L. *Magnetochemistry*; Springer-Verlag: Berlin Heidelberg, 1986.

(18) (a) Kurmoo, M.; Kumagai, H.; Akita-tanaka, M.; Inoue, K.; Takagi, S. *Inorg. Chem.* **2006**, *45*, 1627−1637. (b) Livage, C.; Egger, C.; Férey, G. *Chem. Mater.* **2001**, *13*, 410−414. (c) Feng, S. H.; Xu, R. R. *Acc. Chem. Res.* **2001**, *34*, 239−247. (d) Rabenau, A. *Angew. Chem., Int. Ed. Engl.* **1985**, *24*, 1026−1040.

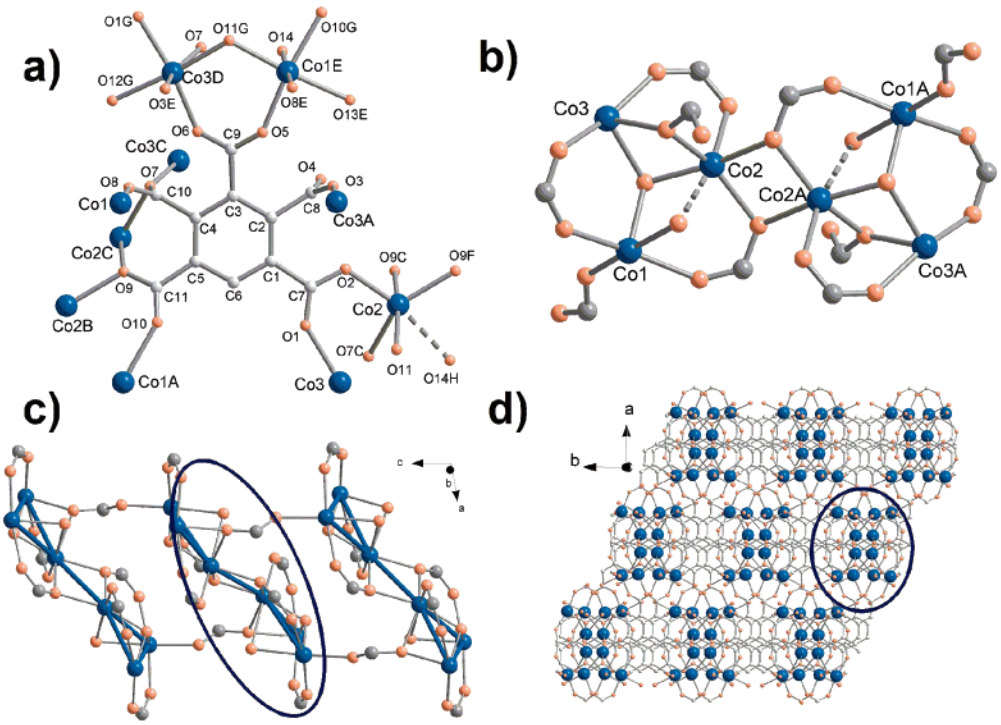

Figure 1. The structure of **1-Co** (and similarly **2-Zn**): (a) the local environments around the BPCA linker and cobalt centers, (b) the hexameric secondary building unit (SBU) of [Co_6], (c) the 1D tapes made of [Co_6] SBUs linked by carboxylic groups along the *c*-axis, and (d) the 3D framework with highlighted 1D tapes. The distance shown with broken lines in parts a and b is relatively long compared to the other distances: 2.348 Å in **1-Co** and much longer, 3.31 Å, in **2-Zn**.

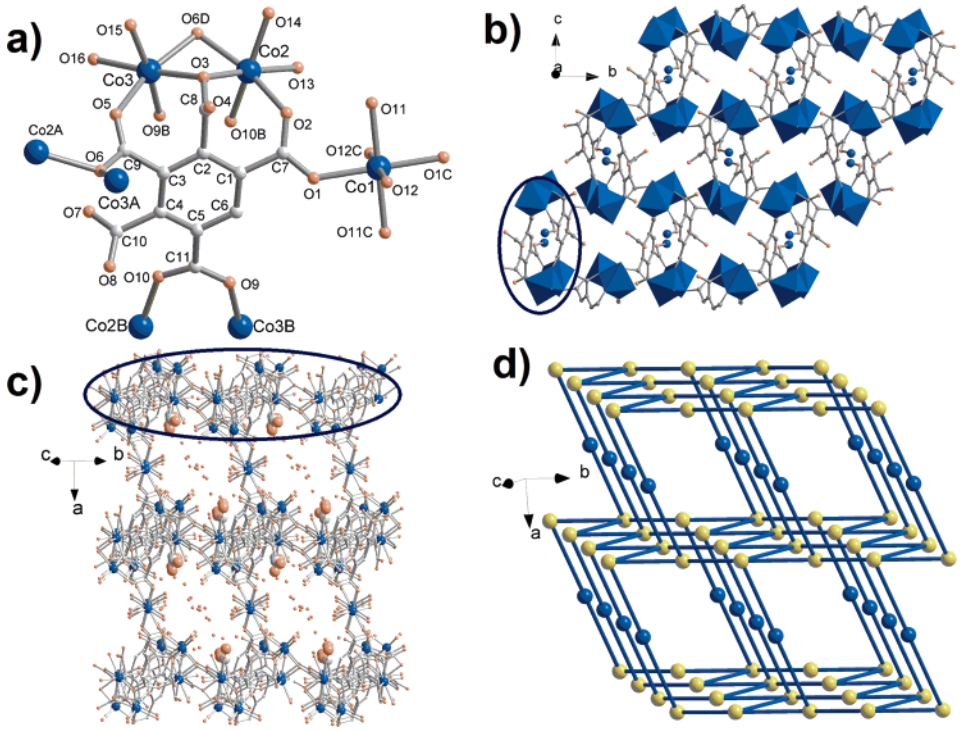

Figure 2. The structure of **3-Co**: (a) the local environments around the BPCA linker and cobalt centers, (b) the 2D layers linked via BPCA groups (Co2 and Co3 are shown as octahedra, Co1 is shown as blue spheres), (c) the 3D structure of the compound made of 2D layers interconnected by Co1 centers (free carboxylates are highlighted), and (d) a simplified linkage of the structure where yellow and blue spheres represent the Co2−Co3 dimers and Co1 centers, respectively.

octahedrally coordinated by six oxygen atoms (two, four, and four atoms are from BPCA linkers for Co1, Co2, and Co3, respectively; the rest are from coordinated water molecules) and have typical Co−O bond lengths in the range of 2.00−2.15 Å (Table 2). The fully deprotonated BPCA ligand is coordinated to seven Co^{2+} centers using only four of its five carboxylate groups, one of the reasons for a more open framework. Three carboxylates, O1−C7−O2, O3−

C8−O4, and O9−C11−O10, link pairs of cobalt atoms in syn−anti, μ_2-O, and syn−syn modes, respectively, while the fourth carboxylate, O5−C9−O6, bridges three cobalt ions in anti−syn/anti mode. The fifth carboxylic group O7−C10−O8 remains noncoordinated as a free functionality in the structure (Figure 2a).

As discussed in the Introduction, free functional groups that are not engaged in metal−linker interactions are of great interest because, if accessible by guest molecules, they may serve as various docking and reaction sites for the guests in the already formed framework. In this particular case, the available carboxylate groups point conveniently toward the water-filled cavities in the structure (Figure 2c) and would be exposed after eventual removal of the lattice water molecules. Unfortunately, however, all attempts to remove the lattice water and preserve the framework were unsuccessful; the structure was damaged despite the very soft conditions of dehydration, such as room temperature and rough vacuum. Clearly some dehydration occurs at these conditions, as evidenced by the change of color from pale red to dark red, but the structure of the product is damaged to such an extent that it diffracted very poorly and could not be characterized any further. Furthermore, the lattice water is so extensively hydrogen bonded with framework oxygen atoms and coordinated water molecule that exchange with other guest molecules is very unlikely. This behavior differs greatly from the observed low-temperature single-crystal-to-single-crystal reversible dehydration under vacuum of a similarly water-stuffed polycarboxylate, that of $[Cu_7Cl_2(THFTC)_2(OH)_4(H_2O)_2](H_2O)_4$, where THFTC is tetrahydrofurantetracarboxylate.[15c] The lattice water in the latter case can be pumped out at room temperature while the single crystallinity is preserved, but the compound does not have free functionalities. Nonetheless, its behavior suggests that the potential for exposing cavities with free functionalities exist and we should explore for more compounds of this type. The best chance for forming such structures seems to belong to small organic linkers with a multitude of functional groups either of the same or different kind.

The distances between the carboxylate-bridged Co atoms in **3-Co** are in the range 3.15−5.84 Å. The two octahedra centered by Co2 and Co3 share an edge of two oxygen atoms (from two different carboxylate groups) and can be viewed as a dimeric SBU. The SBUs form 1D chains along the *b*-axis, and the chains are linked along the *c*-axis by BPCA groups to form brick-wall-type 2D layers of (6,3) topology parallel to the *bc*-plane (Figure 2b). The layers are connected into a three-dimensional framework via the Co1 centers, which bond along the [101] direction to SBUs from different layers (Figure 2c,d). This connectivity results in infinite galleries along the [011] direction that hold the lattice water molecules hydrogen bonded to carboxylic groups and to coordinated water molecules. As can be seen from the simplified topology depicted in Figure 2d, the SBUs are four-connected nodes and the whole structure can be described as a three-dimensional brick wall structure.

Magnetic Properties of 1-Co. The temperature dependence of the magnetic susceptibility of **1-Co** measured at 1 kOe from 2 to 300 K is depicted in Figure 3. The χT value of 3.03 $cm^3 \cdot K \cdot mol^{-1}$ at 300 K (calculated per Co^{2+} cation) decreases monotonously to a shallow minimum at about 14 K. Below this temperature, it increases slightly, peaking at 5.8 K, and then drops again toward zero. The Curie−Weiss fit of the inverse magnetic susceptibility above 50 K provides a Curie constant $C = 3.35$ $cm^3 \cdot K \cdot mol^{-1}$ and Weiss temperature $\theta = -29.9$ K. The effective magnetic moment that corresponds to this Curie constant, $\mu_{eff} = 5.18$ μ_B, is significantly higher than the calculated spin-only value of 3.87 μ_B expected for a weak-field d^7 metal center and indicates relatively strong spin−orbit coupling. Such a moment, however, is very typical for octahedrally coordinated Co^{2+} ions with $^4T_{1g}$ electronic state, for which the observed moments typically fall in the range 4.3−5.2 μ_B.[19]

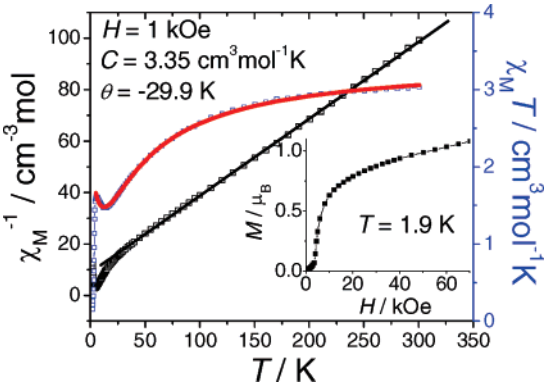

Figure 3. The temperature dependence of χ^{-1} and χT for **1-Co** measured at 1 kOe. The black line is the Curie−Weiss fit of χ^{-1} above 50 K, while the red line corresponds to the fit of χT with the function $\chi T = C_1 \exp(J_\alpha/k_BT) + C_2 \exp(J_\beta/k_BT)$. The inset shows the field dependence of the magnetization at 1.9 K.

The existence of tightly interconnected Co-centers within the $[Co_6]$ hexameric SBUs as well as between the SBUs linked by carboxylic groups at close proximity in the chains implies that its magnetic properties at high temperatures will be dominated by magnetic interactions within the SBUs and between the SBUs in the chains. Unfortunately, this amounts to a very large number of available magnetic pathways and a very complex magnetic structure that make impossible the eventual extraction of coupling parameters. Nonetheless, one conclusion that can be made is that, according to the significantly negative Weiss constant, antiferromagnetic interactions between the magnetic centers dominate the magnetic exchange at higher temperatures, although strong spin−orbit coupling may contribute to the negative number as well.

The situation is somewhat different at lower temperatures, where the observed slight increase of χT suggests the presence of either ferromagnetic coupling or spin-canting. The combined magnetic interactions can be approximated with the following simple phenomenological equation:

$$\chi T = C_1 \exp(J_\alpha/k_BT) + C_2 \exp(J_\beta/k_BT) \qquad (1)$$

(19) Carlin, R. L. *Magnetochemistry*; Springer-Verlag: Berlin, 1986; pp 53 and 65.

[20] The two coupling parameters J_α and J_β, correspond to the two different types of interactions, i.e., antiferro- and ferromagnetic, respectively. Thus, the spin−orbital coupling and the antiferromagnetic interactions that are predominant at higher temperatures are represented by a negative J_α, while a positive J_β corresponds to the weaker ferromagnetic interaction at very low temperatures. The sum of C_1 and C_2 should roughly equal the Curie constant. The best fit of the experimental data down to 5 K (Figure 3) gives $C_1 = 2.06(1)$ cm^3·K·mol^{-1}, $J_\alpha = -36.0(5)$ cm^{-1}, $C_2 = 1.32(1)$ cm^3·K·mol^{-1}, and $J_\beta = 0.80(4)$ cm^{-1}. Thus, $C_1 + C_2 = 3.38$ cm^3·K·mol^{-1}, and this is very close to the measured Curie constant of 3.35 cm^3·K·mol^{-1}. Notice that the positive J_β is a very small number compared to J_α, and this is in agreement with the much weaker ferromagnetic interaction at low temperatures. It should be pointed out that eq 1 was developed and is typically used for evaluation of spin−orbit and intrachain coupling in regular 1D chains through the noncritical scaling approach.[20] Although compound **1-Co** can be roughly treated as a 1D-like system (very weak or nonexistent magnetic coupling via the carbon backbone of the BPCA ligand), the values derived for J_α and J_β are only very approximate estimations for the effective coupling.

The isothermal field dependence of the magnetization at 1.9 K and fields of up to 70 kOe showed an obvious *S*-type shape (Figure 3). The magnetization increases slowly in the regions 0−3.5 and 10−70 kOe, but turns up very sharply in the middle region of 3.5−10 kOe. Such behavior is very typical for a metamagnetic transition with two ferromagnetic subnetworks weakly coupled antiferromagnetically.[17,21] The magnetization of 1.08 μ_B at 70 kOe and 1.9 K is far below the normally observed value of 2−3 μ_B for an isotropic high-spin Co^{2+} [17] and might originate from the existence of strong anisotropy of the antiferromagnetic ground state. The critical field H_C for the metamagnetic transition at 1.9 K is deduced to be about 4 kOe from the peak in the d*M*/d*H* curve (Figure 4). These observations prompted more *M*(*H*) measurements at different temperatures in the range of 1.9−4 K in order to obtain the *H*−*T* magnetic phase diagram for this compound. As can be seen from Figure 4, the *S*-shape abnormality of the curve becomes less pronounced upon increasing the temperature and disappears completely at 4 K. The differentials of these curves (inset in Figure 4) show peaks that shift to lower fields as the temperature increases. These peaks give a set of (*H*,*T*) points that correspond to the phase boundary in the magnetic phase diagram (vide post).

In addition to the isothermal *M*(*H*) measurements, the metamagnetic transition was confirmed also by a series of low-temperature *M*(*T*) measurements carried out at 10 different external fields between 20 and 6000 Oe (Figure 5). The corresponding curves at low fields of below 5000 Oe show well-defined peaks that shift to lower temperatures as the field increases, while the peaks disappear when the field reaches 6000 Oe. The differentials of these curves [d(*MT*/*H*)/d*T* vs *T*, inset in Figure 5] provide another set of (*H*,*T*) points in the magnetic phase diagram of **1-Co**. When plotted, as shown in Figure 6, the two sets of points present a fairly complete boundary between the antiferromagnetic and paramagnetic forms of the compound. This boundary gives an estimated critical temperature of $T_N = 3.8$ K.

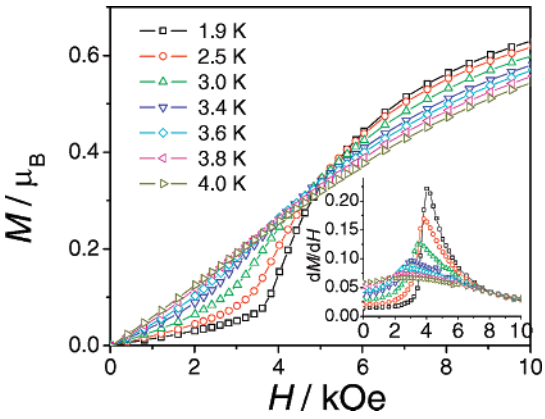

Figure 4. The field dependence of the magnetization of **1-Co** measured at different temperatures and their derivatives shown in the inset.

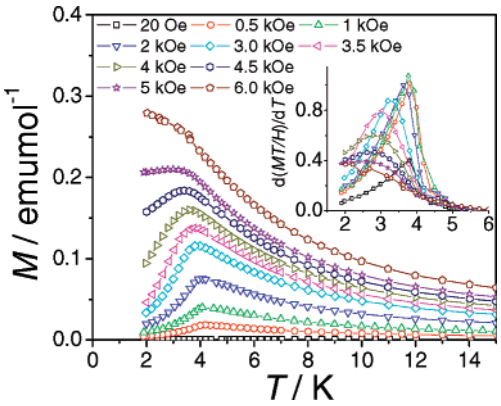

Figure 5. The temperature dependence of the magnetization of **1-Co** measured at different fields and their derivatives [d(*MT*/*H*)/d*T* vs *T*] shown in the inset.

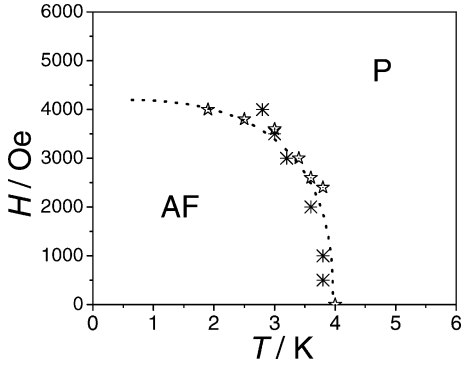

Figure 6. The *H*−*T* magnetic phase diagram for **1-Co**. The stars and crosses are from the *M*(*H*) and *M*(*T*) curves, respectively.

Magnetic Properties of 3-Co. Unlike **1-Co**, the magnetic properties of this compound are quite ordinary (Figure 7). Its χT drops down very slowly from 3.28 cm^3·K·mol^{-1} at

(20) (a) Miller, J. S.; Drillon, M. *Magnetism: Molecules to Materials*; Wiley-VCH: Weinheim, 2005; Vol. V, chapter 10, p 347. (b) Drillon, M.; Panissod, P.; Rabu, P.; Souletie, J.; Ksenofontov, V.; Gütlich, P. *Phys. Rev. B* **2002**, *65*, 104404. (c) Souletie, J.; Drillon, M.; Rabu, P.; Pati, S. K. *Phys. Rev. B* **2004**, *70*, 054410. (d) Souletie, J.; Rabu, P.; Drillon, M. *Phys. Rev. B* **2005**, *72*, 214427. (e) Rueff, J. M.; Masciocchi, N.; Rabu, P.; Sironi, A.; Skoulios, A. *Eur. J. Inorg. Chem.* **2001**, 2843−2848.

(21) Carlin, R. L.; van Duyneveldt, A. J. *Acc. Chem. Res.* **1980**, *13*, 231−236.

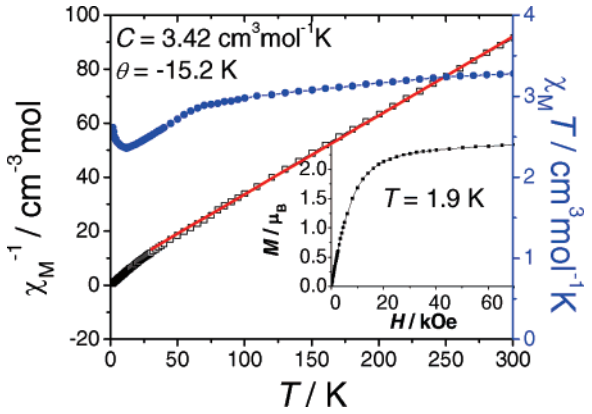

Figure 7. The temperature dependence of χ^{-1} with a Curie−Weiss fit (red line) and χT for **3-Co**. The inset shows the field dependence of the magnetization at 1.9 K.

300 K to a shallow minimum at 11.5 K and then increases slightly down to 2 K. The Curie−Weiss fit of χ^{-1} above 50 K results in a Curie constant $C = 3.42$ cm^3·K·mol^{-1} and a Weiss constant $\theta = -15.2$ K. As for many Co^{2+} compounds, substantial spin−orbit coupling contributes to the high χT and C values. The combination of negative θ and increasing χT below 11 K suggests that both antiferromagnetic and ferromagnetic interactions are possible, most likely due to the multitude of possible magnetic exchange pathways in **3-Co**. The $M(H)$ curve at 1.9 K (inset in Figure 7) shows a typical paramagnetic behavior without long-range magnetic ordering, i.e., a featureless increase with the field until reaching the saturation moment of $M_s = 2.42\ \mu_B$ at 70 kOe for Co^{2+} (expected range of $2-3\ \mu_B$).[17] This was further confirmed by the observed featureless $M(T)$ curve obtained at a very low field of 20 Oe (field-cooled) and temperature range 2−30 K (Figure S1 in the Supporting Information).

Summary

Evidently, small-ring polycarboxylates, such as the benzenepentacrboxylate utilized here, have the potential to generate novel frameworks with promising structural features and properties. Examples are the free carboxylic group in **3-Co** and the interesting magnetic properties of **1-Co**, but there are many other unknown and unpredictable possibilities. The three new compounds reported here fill a blank region in the area of metal−organic frameworks that utilize benzene-based polycarboxylates $C_6H_{6-n}(COO)_n^{n-}$ as linkers, in this case linkers with $n = 5$. We believe that these results strongly justify further work on systems with polycarboxylate linkers and transition metals. Furthermore, inclusion of other components such as auxiliary bridging or terminal coligands and templating molecules may lead to even more interesting and multifunctional metal−organic frameworks.

Acknowledgment. We thank the National Science Foundation for the financial support of this research (DMR-0600320) and for the purchase of a Bruker APEX II diffractometer (CHE-0443233).

Supporting Information Available: X-ray crystallographic CIF files for all compounds in this work and the $M(T)$ curve for **3-Co** at 20 Oe. This material is available free of charge via the Internet at http://pubs.acs.org.

IC701893Z